



1 **REVIEW ARTICLE: THE USE OF REMOTELY PILOTED AIRCRAFT SYSTEMS**  
2 **(RPAS) FOR NATURAL HAZARDS MONITORING AND MANAGEMENT**

3 Daniele Giordan<sup>1</sup>, Yuichi Hayakawa<sup>2</sup>, Francesco Nex<sup>3</sup>, Fabio Remondino<sup>4</sup>, Paolo Tarolli<sup>5</sup>

4 <sup>1</sup>Istituto di Ricerca per la Protezione Idrogeologica, Consiglio Nazionale delle Ricerche, Italy

5 <sup>2</sup>Center for Spatial Information Science, The University of Tokyo, Japan

6 <sup>3</sup>University of Twente, Faculty of Geo-Information Science and Earth Observation (ITC), The Netherlands

7 <sup>4</sup>3D Optical Metrology (3DOM) Unit, Bruno Kessler Foundation (FBK), Trento, Italy

8 <sup>5</sup>Department of Land, Environment, Agriculture and Forestry, University of Padova, Italy

9

10 **ABSTRACT**

11

12 The number of scientific studies that consider possible applications of Remotely Piloted Aircraft Systems  
13 (RPAS) for the management of natural hazards effects and the identification of occurred damages are  
14 strongly increased in last decade. Nowadays, in the scientific community, the use of these systems is not a  
15 novelty, but a deeper analysis of literature shows a lack of codified complex methodologies that can be  
16 used not only for scientific experiments but also for normal codified emergency operations. RPAS can  
17 acquire on-demand ultra-high resolution images that can be used for the identification of active processes  
18 like landslides or volcanic activities but also for the definition of effects of earthquakes, wildfires and floods.  
19 In this paper, we present a review of published literature that describes experimental methodologies  
20 developed for the study and monitoring of natural hazards.

21

22 **1. INTRODUCTION**

23

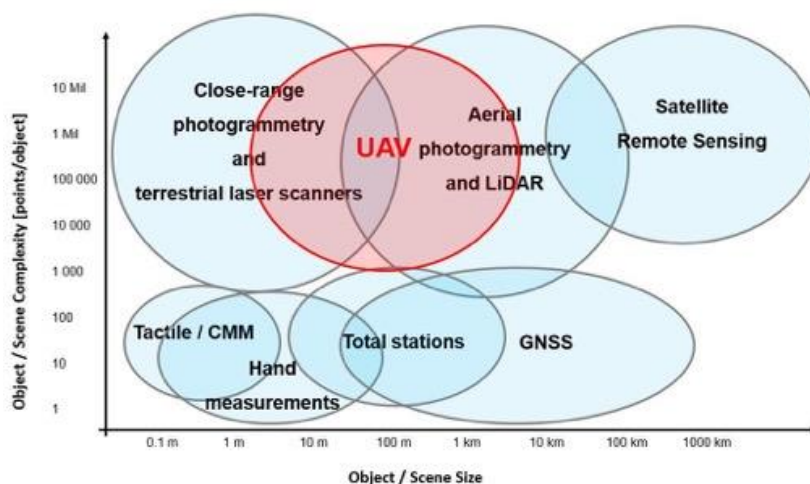
24 In last three decades, the number of natural disasters showed a positive trend with an increase in the  
25 number of affected populations. Disasters not only affected the poor and characteristically more vulnerable  
26 countries but also those thought to be better protected. Annual Disaster Statistical Review describes recent  
27 impacts of natural disasters over population and reports 376 natural triggered disasters in 2015 (ADSR,  
28 2015). This is less than the average annual disaster frequency observed from 2005 to 2014 (380), however  
29 natural disasters is still responsible for a high number of casualties (22,765). In 2015, hydrological disasters  
30 (175) had the largest share in natural disaster occurrence (46.5%), followed by meteorological disasters  
31 (127; 33.8%), climatological disasters (45; 12%) and geophysical disasters (29; 7.7%) (ADSR, 2015). To face  
32 these disasters, one of the most important solutions is the use of systems able to provide an adequate level  
33 of information for correctly understanding these events and their evolution. In this context, survey and  
34 monitoring of natural hazards gained in importance. In particular, during the emergency phase it is very  
35 important to evaluate and control the phenomenon evolution, preferably operating in near real time or  
36 real time, and consequently, use this information for a better risk scenario assessment. The available  
37 acquired data must be processed rapidly to ensure the emergency services and decision makers promptly.



38 Recently, the use of remote sensing (satellite and airborne platform) in the field of natural hazards and  
39 disasters has become common, also supported by the increase in geospatial technologies and the ability to  
40 provide and process up-to-date imagery (Joyce et al., 2009; Tarolli, 2014). Remotely sensed data play an  
41 integral role in predicting hazard events such as floods and landslides, subsidence events and other ground  
42 instabilities. Because their acquisition mode and capability for repetitive observations, the data acquired at  
43 different dates and high spatial resolution can be considered as an effective complementary tool for field  
44 techniques to derive information on landscape evolution and activity over wide areas.

45 In the contest of remote sensing research, recent technological developments have increased in the field of  
46 Remotely Piloted Aircraft Systems (RPAS) becoming more common and widespread in civil and commercial  
47 context (Boccardo et al., 2008). In particular, the development of photogrammetry and technologies  
48 associated (i.e. RLS digital cameras and GNSS/INS systems) allow to use of RPAS platforms in various  
49 applications as alternative to the traditional remote sensing method for topographic mapping or detailed  
50 3D recording of ground information and a valid complementary solution to terrestrial acquisitions too (Nex  
51 and Remondino, 2014) (Fig.1).

52 RPAS systems present some advantages in comparison to traditional platforms and, in particular, they  
53 could be competitive thanks to their versatility in the flight execution. Mini/micro RPAS are the most  
54 diffused for civil purposes, and they can fly at low altitudes according to limitations defined by national  
55 aviation security agencies. Stöcker et al. (2017) published a review of different state regulations that are  
56 characterized by several differences regarding requirements, distance from the takeoff and maximum  
57 altitude. Another important added value of RPAS is their adaptability that allows their use in various  
58 typologies of missions, and in particular for monitoring operations in remote and dangerous areas. The  
59 possibility to carry out flight operations at lower costs compared to ones required by traditional aircraft is  
60 also a fundamental advantage. Limited operating costs make these systems also convenient for multi-  
61 temporal applications where it is often necessary to acquire information on an active process (like a  
62 landslide) over the time.



63

64 Figure 1. Available geomatics techniques, sensors, and platforms for topographic mapping or detailed 3D  
65 recording of ground information, according to the scene dimensions and complexity (modified from Nex  
66 and Remondino, 2014).

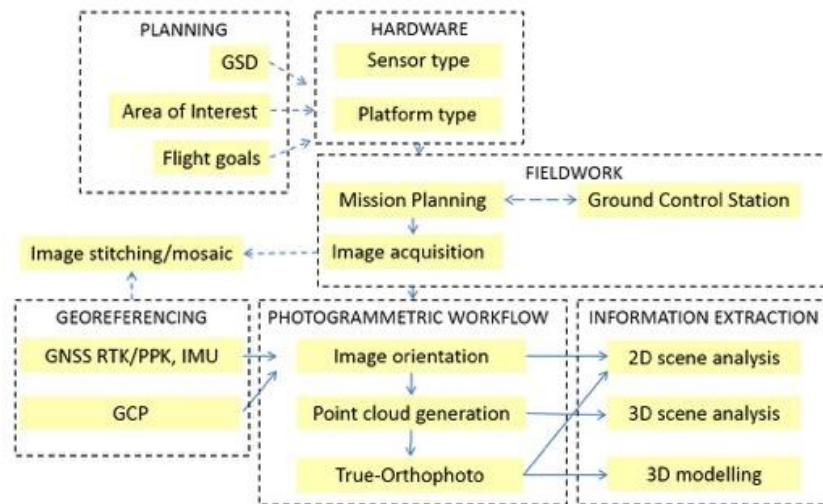


67 RPASs are used in several fields as agriculture, forestry, archaeology and architecture, traffic monitoring,  
68 environment and emergency management. In particular, in the field of emergency assistance and  
69 management, RPAS platforms are used to reliably and fast collect data of inaccessible areas. Collected data  
70 can be mostly images but also gas concentrations or radioactivity levels as demonstrated by the tragic  
71 event in Fukushima (Sanda et al., 2015; Martin et al., 2016). Focusing on image collection, they can be used  
72 for early impact assessment, to inspect collapsed buildings and to evaluate structural damages (Chou et al.  
73 2010; Molina et al. 2012; Murphy et al., 2008; Pratt et al., 2009). Environmental and geological monitoring  
74 can profit from fast multi-temporal acquisitions delivering high-resolution images (Thamm and Judex 2006;  
75 Niethammer et al. 2010). RPAS can be considered a good solution also for mapping and monitoring  
76 different active processes at the earth surface such as: glaciers (Immerzel et al., 2014, Ryan et al., 2015),  
77 Antarctic moss beds (Lucieer et al., 2014b), costal areas (Delacourt et al., 2009; Klemas, 2015), river  
78 morphodynamic (Juad et al., 2016) and river channel vegetation (Dunford et al., 2009).

79 The incredible diffusion of RPAS has pushed many companies to develop dedicated sensors for these  
80 platforms. Besides the conventional RGB cameras other camera sensors are nowadays available on the  
81 market. Multi- and hyper-spectral cameras, as well as thermal sensors, have been miniaturized and  
82 customized to be hosted on many platforms.

83 The general workflow of a UAV acquisition is presented in Figure 2 below. The resolution of the images, the  
84 extension of the area as well as the goal of the flight are the main constraints that affect the selection of  
85 the platform and the typology of the sensor. Large areas can be flown using fixed wing (or hybrid) solutions  
86 able to acquire nadir images in a fast and efficient way. Small areas or complex objects (like steep slopes or  
87 buildings) should be acquired using rotor RPAS as they are usually slower but they allow the acquisition of  
88 oblique views. If the information different from the visible band is needed, the RPAS can host one or more  
89 sensors acquiring in different bands. The flight mission can be planned using dedicated software: they  
90 range from simple apps installed on smartphones in the low-cost solutions, to laptops connected to  
91 directional antennas and remote controls for the most sophisticated platforms. According to the typology  
92 of the platform, different GNSS and IMU can be installed. Low-cost solutions are usually able to give  
93 positions with few meters accuracy and need GCP (Ground Control Points) to geo-reference the images. On  
94 the other hand, most expensive solutions install double frequency GNSS receivers with the possibility to get  
95 accurate geo-referencing thanks to RTK or PPK corrections. If a quick mapping is needed, the information  
96 delivered by the navigation system can be directly used to stitch the images and produce a rough image  
97 mosaicking. In the alternative, the typical photogrammetric process is followed: (i) image orientation, (ii)  
98 DSM generation and (iii) orthophoto generation. The position (geo-referencing) and the attitude (rotation  
99 towards the coordinates system) of each acquisition is obtained by estimating the image orientation. In the  
100 dense point cloud generation, 3D point clouds are generated from a set of images, while the orthophoto is  
101 generated in the last step combining the oriented images projected on the generated point cloud, leading  
102 to orthorectified images. Point clouds can be very often converted in Digital Surface Models (DSM), and  
103 Digital Terrain Models (DTM) can be extracted removing the off ground regions (mainly buildings and  
104 trees).

105 The outputs from the last two steps (point clouds and true-orthophotos) as well as the original images are  
106 very often used as input in the scene understanding process: classification of the scene or extraction of  
107 features (i.e. objects) of interest using machine learning techniques are the most common applications. 3D  
108 models can also be generated using the point cloud and the oriented images to texturize the model.



109

110

Figure 2. Acquisition and processing of RPAS images: general workflow

111 In this paper, the authors present an analysis and evaluation concerning the use of RPAS as alternative  
 112 monitoring technique to the traditional methods, relating to the natural hazard scenarios. The main goal is  
 113 to define and test the feasibility of a set of methodologies that can be used in the monitoring and mapping  
 114 activities. The study is focused in particular on the use of mini and micro RPAS systems (Table 1). The  
 115 following table listed the technical specifications of these two RPAS categories, again based on the current  
 116 classification by UVS (Unmanned Vehicle Systems) International. Most of the mini or micro RPAS systems  
 117 available integrate a flight control system, which autonomously stabilizes these platforms and enables the  
 118 remotely controlled navigation. Additionally, they can integrate an autopilot, which allows an autonomous  
 119 flight based on predefined waypoints. For the monitoring and mapping applications, mini- or micro RPAS  
 120 systems are very useful as cost-efficient platforms for capturing real-time close-range imagery. These  
 121 platforms can reach the area of investigation and take several photos and videos from several points and  
 122 different angles of view. For mapping applications, it is also possible to use this flight control data to geo-  
 123 register the captured payload sensor data like still images or video streams (Eugster and Nebiker, 2008).

124

Table 1. Classification of mini and micro UAV systems

Category	Max. Take Of Weight	Max. Flight Altitude	Endurance	Data Link Range
Mini	<30kg	150-300m	<2h	<10km
Micro	<5Kg	250m	1h	<10km

125

## 126 2. USE OF RPAS FOR NATURAL HAZARDS DETECTION AND MONITORING

127

128 According to the definitions used by Annual Disaster Statistical Review (ADSR, 2015), the paper considers in  
 129 particular phenomena that can be analyzed using RPAS and in particular: i) landslides, ii) floods iii)  
 130 earthquakes v) volcanic activity vi) wildfires. For each considered category of natural hazard, the paper



131 presents an analysis of published methodologies and provide results, underlining strengths and limitations  
132 in the use of RPAS.

133

## 134 2.1 Landslides

135 Landslides are one of the major natural hazards that produce each year enormous property damage  
136 regarding both direct and indirect costs. Landslides are rock, earth or debris flows on slopes due to gravity.  
137 The event can be triggered by a variety of external elements, such as intense rainfall, water level change,  
138 storm waves or rapid stream erosion that cause a rapid increase in shear stress or decrease in shear  
139 strength of slope-forming materials. Moreover, the pressures of increasing population and urbanization,  
140 human activities such as deforestation or excavation of slopes for road cuts and building sites, etc., have  
141 become important triggers for landslide occurrence. Because the factors affecting landslides can be  
142 geophysical or human-made, they can occur in developed and undeveloped areas.

143 In the field of natural hazards, the use of RPAS for landslides study and monitoring represents one of the  
144 most common applications. The number of papers that present case studies or possible methodologies  
145 dedicated to this topic has strongly increased in last few years and now the available bibliography offers a  
146 good representation of possible approaches and technical solutions.

147 When a landslide occurs, the first information to be provided is the extent of the area affected by the event  
148 (figure 3). The landslide impact extent is usually done based on detailed optical images acquired after the  
149 event. From these acquisitions, it is possible to derive Digital Elevation Models (DEMs) and orthophotos  
150 that allow detecting main changes in geomorphological figures. In this scenario, the use of the mini-micro  
151 RPAS is practical for small areas and optimal for landslides that often cover an area that range from less  
152 than one square kilometres up to few square kilometres. Ultra-high resolution images acquired by RPAS can  
153 support the definition not only of the identification of studied landslide limit, but also the identification and  
154 mapping of main geomorphological features (Fiorucci et al., 2017). Furthermore, a sequence of RPAS  
155 acquisitions over the time can provide useful support for the study of the gravitational process evolution.

156 According to Scaioni et al. (2014), applications of remote sensing for landslides investigations can be  
157 divided into three classes: i) landside recognition, classification and post-event analysis, ii) landslide  
158 monitoring, iii) landslide susceptibility and hazard assessment.

159

160



161

162 Figure 3. Example of RPAS image of a rockslide occurred on a road. The image was acquired after the  
163 rockslide occurred in 2014 in San Germano municipality (Piemonte region, NW Italy). As presented in  
164 Giordan et al. (2015a), a multi-rotor of local Civil Protection Agency was used to evaluate occurred damages  
165 and residual risk. RPAS images can be very useful to have a representation from a different point of view of  
166 the occurred phenomena. Even not already processed using SFM applications, this dataset can be very  
167 useful for decision makers to define the strategy for the management of the first phase of emergency.

168

### 169 2.1.1 Landslides recognition

170 The identification and mapping of landslides are usually performed after intense meteorological events that  
171 can activate or reactivate several gravitational phenomena. The identification and mapping of landslides  
172 can be organized in landslides event maps. Landslides event mapping is a well-known activity obtained  
173 through field surveys (Santangelo et al., 2010), visual interpretation of aerial or satellite images (Brardinoni  
174 et al., 2003; Ardizzone et al., 2013) combined analysis of LiDAR DTM and images (Van Den Eeckhaut et al.,  
175 2007; Haneberg et al., 2009; Giordan et al., 2013; Razak et al., 2013; Niculita et al., 2016). The use of RPAS  
176 for the identification and mapping of a landslide has been described by several authors (Niethammer et al  
177 2009; Niethammer et al 2010; Rau et al., 2011; Carvajal et al., 2012; Travelletti et al., 2012; Torrero et al.,  
178 2015; Casagli et al., 2017). Niethammer et al. (2009) showed how RPAS could be considered a good solution  
179 for the acquisition of ultra-high resolution images with low-cost systems. Fiorucci et al. (2017) compared  
180 the results of the landslide limit mapped using different techniques and found that satellite images can be  
181 considered a good solution for the identification and map of landslides over large areas. On the contrary, if  
182 the target of the study is the definition of landslide's morphological features, the use of more detailed RPAS  
183 images seemed to be the better solution. As suggested by Walter et al., (2009) and Huang et al., (2017)  
184 one of the most critical elements for a correct georeferencing of acquired images are the use of Ground  
185 Control Points (GCPs). The in situ installation and positioning acquisition of GCPs can be an important  
186 challenge in particular in dangerous areas as active landslides. Very often, GCPs are not installed in the



187 most active part of the slide but on stable areas. This solution can be safer for the operator, but it can also  
188 reduce the accuracy of the final reconstruction.

189 Another parameter that can be considered during the planning of the acquisition phase is the morphology  
190 of the studied area. According to with Giordan et al., (2015b), slope materials and gradient can affect the  
191 flight planning and the approach used for the acquisition of the RPAS images. Two possible scenarios can be  
192 identified: i) steep to vertical areas (>40°); ii) slopes with gentle to moderate slopes (<40°). In the first case,  
193 the use of multi-copters with oblique acquisitions is often the best solution. On the contrary, with more  
194 gentle slopes, the use of fixed-wing systems can assure the acquisition of wider areas.

195

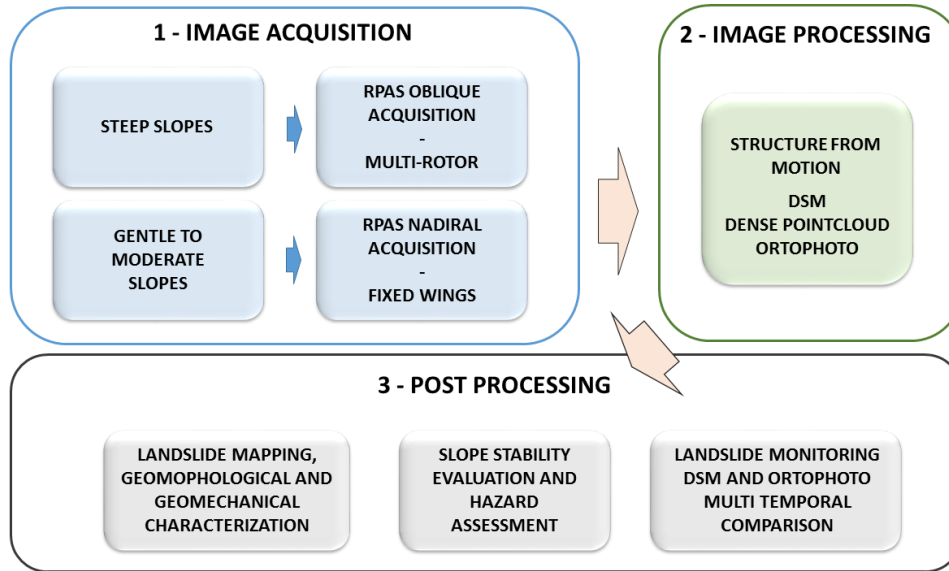
### 196 **2.1.2 Landslides monitoring**

197 The second possible field of application of RPAS is the use of multi-temporal acquisitions for landslides  
198 monitoring. This topic has been described by several authors (Turner and Lucieer 2013, Travelletti et al.,  
199 2012, Lucieer et al. 2014a; Turner et al., 2015; Marek et al., 2015). In these works, numerous techniques  
200 based on the multi-temporal comparison of RPAS datasets for the definition of the evolution of landslides  
201 have been presented and discussed. Niethammer et al. (2010 and 2012) described how the position change  
202 of geomorphological features (in particular fissures) could be considered for a multi-temporal analysis with  
203 the aim of the characterization of the landslide evolution. Travelletti et al. (2012) introduced the possibility  
204 of a semi-automatic image correlation to improve this approach. The use of image correlation techniques  
205 has been also described by Lucieer et al. (2014a) who demonstrated that COSI-Corr (Co-registration of  
206 Optically Sensed Imaged and Correlation - LePrince et al. 2007, 2009; Ayoub et al., 2009) can be adopted  
207 for the definition of the surface movement of the studied landslide. A possible alternative solution is the  
208 multi-temporal analysis of the use of DSMs. The comparison of digital surface models can be used for the  
209 definition of volumetric changes caused by the evolution of the studied landslide. The acquisition of these  
210 digital models can be done with terrestrial laser scanners (Baldo et al., 2009) or airborne LiDAR (Giordan et  
211 al., 2013). Westoby et al. (2012) emphasized the advantages of RPAs concerning terrestrial laser scanner,  
212 which can suffer from line-of-sight issues, and airborne LiDAR, which are often cost-prohibitive for  
213 individual landslide studies. Turner et al. (2015) stressed the importance of a good co-registration of multi-  
214 temporal DSM for good results that could decrease the accuracy of results. The use of benchmarks in areas  
215 not affected by morphological changes can be used for a correct calibration of rotational and translation  
216 parameters.

217

### 218 **2.1.3 Landslides susceptibility and hazard assessment**

219 Landslides susceptibility and hazard assessment are often performed at basin scale (Guzzetti et al., 2005)  
220 using different remote sensing techniques (Van Westen et al., 2008). The use of RPAS can be considered for  
221 single case study applications to help decision makers in the identification of the landslide damages and the  
222 definition of residual risk (Giordan et al., 2015a). Saroglou et al., (2017) presented the use of RPAS for the  
223 definition of trajectories of rock falls prone areas. Salvini et al. (2017) and Török et al., (2017) described the  
224 combined use of TLS and RPAs for hazard assessment of steep rock walls. All these papers considered the  
225 use of RPAS as a valid solution for the acquisition of DSM over sub-vertical areas. Török et al., (2017) and  
226 Tannant et al., 2017 also described in their manuscripts how RPAS DSMs can be used for the evaluation of  
227 slope stability using numerical modelling.



228

229

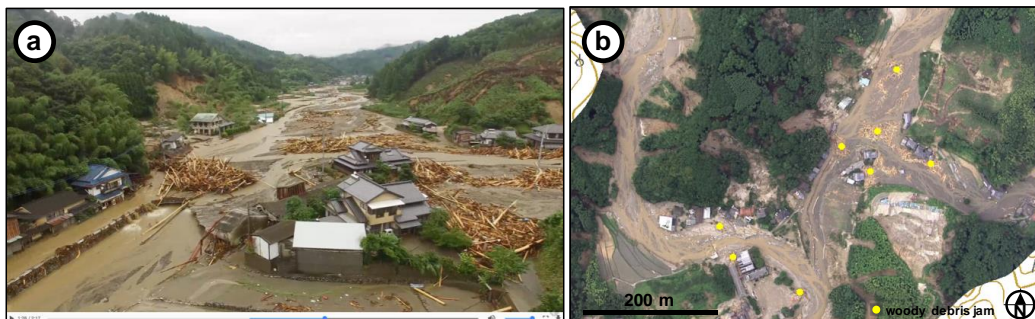
230 Figure 4. Acquisition, processing and post-processing of RPAS images applied to i) landslides recognition, ii)  
 231 hazard assessment and iii) slope evolution monitoring

232

### 233 2.2 Floods

234 Disastrous floods in urban, lowland areas often cause fatalities and severe damage to the infrastructure.  
 235 Monitoring the flood flow, assessment of the flood inundation areas and related damages, post-flood  
 236 landscape changes, and pre-flood prediction are therefore seriously required. Among various scales of  
 237 approaches for flood hazards (Sohn et al., 2008), the RPAS has been adopted for each purpose of the flood  
 238 damage prevention and mitigation because it has an ability of quick measurement at a low cost (DeBell et  
 239 al., 2016; Nakamura et al., 2017). Figure 5 shows an example of the use of RPAS for prompt damage  
 240 assessment by a severe flood occurred on early July 2017 at northern Kyushu area, southwest Japan. The  
 241 Geospatial Information Authority of Japan (GSI) utilized an RPAS for the post-flood video recording and  
 242 photogrammetric mapping of the damaged area with flood flow and large woody debris.

243







244 Figure 5. Image captures of flood hazard using RPAS just after the 2017 Northern Kyushu Heavy Rain in the  
245 early July (southwest Japan), provided by GSI. (a) A screenshot of the aerial video of a flooded area along  
246 the Akatani River, Asakura City in Fukuoka Prefecture. (b) Orthorectified image of the damaged area.  
247 Locations of woody debris jam are mapped and shown on the online map (GSI, 2017). The video and map  
248 products are freely provided (compatible with Creative Commons Attribution 4.0 International).

249

### 250 **2.2.1. Potential analysis of flood inundation**

251 The risk assessments of flood inundation before the occurrence of a flood is crucial for the mitigation of the  
252 flood-disaster damages. RPAS is capable of providing quick and detailed analysis of the land surface  
253 information including topographic, land cover, and land use data, which are often incorporated into the  
254 hydrological modelling for the flood estimate (Costa et al., 2016). As a pre-flood assessment, Li et al. (2012)  
255 explored the area around an earthquake-derived barrier lake using an integrated approach of remote  
256 sensing including RPAS for the hydrological analysis of the potential dam-break flood. They proposed a  
257 technical framework for the real-time evacuation planning by accurately identifying the source water area  
258 of the dammed lake using a RPAS, followed by along-river hydrological computations of inundation  
259 potential. Tokarczyk et al. (2015) showed that the UAV-derived imagery is useful for the rainfall-runoff  
260 modelling for the risk assessment of floods by mapping detailed land-use information. As a key input data,  
261 high-resolution imperviousness maps were generated for urban areas from UAV imagery, which improved  
262 the hydrological modelling for the flood assessment. Zazo et al. (2015) and Şerban et al. (2016)  
263 demonstrated hydrological calculations of the potentially flood-prone areas using UAV-derived 3D models.  
264 They utilized 2D cross profiles derived from the 3D model for the hydrological modelling.

265

### 266 **2.2.2. Flood monitoring**

267 Monitoring of the ongoing flood is potentially important for the real-time evacuation planning. Le Coz et al.  
268 (2016) mentioned that the movies captured by a RPAS, which can be operated by not only research  
269 specialists but also general non-specialists, is potentially useful for the quantitative monitoring of floods  
270 including flow velocity estimate and flood modelling. This can also contribute to the crowdsourced data  
271 collection for flood hydrology as the citizen science. In case of flood monitoring, however, areas under  
272 water is often problematic by image-based photogrammetry because the bed is not often fully seen in  
273 aerial images. If the water is clear enough, bed images under water can be captured, and the bed  
274 morphology can be measured with additional corrections of refraction (Tamminga et al., 2015; Woodget et  
275 al., 2015), but the flood water is often unclear because of the abundant suspended sediment and disturbing  
276 flow current. Another option is the fusion of different datasets using a sonar-based measurement for the  
277 water-covered area, which is registered with the terrestrial datasets (Flener et al., 2013; Javernick et al.,  
278 2014). Image-based topographic data of water bottom by unmanned underwater vehicle (UUV, also known  
279 as an autonomous underwater vehicle, AUV) can also be another option (e.g., Pyo et al., 2015), although  
280 such the application of UUV to flooding has been limited.

281 Not only the use of topographic datasets derived from SfM-MVS photogrammetry, the use of orthorectified  
282 images concurrently derived from the RPAS-based aerial images is advantageous for the assessment of  
283 hydrological observation and modelling of floods. Witek et al. (2014) developed an experimental system to  
284 monitor the stream flow in real time for the prediction of overbank flood inundation. The real-time



285 prediction results are also visualized online with a web map service with a high-resolution image (3 cm/pix).  
286 Feng et al. (2015) reported that the accurate identification of inundated areas is feasible using UAV-derived  
287 images. In their case, deep learning approaches of the image classification using optical images and texture  
288 by UAV successfully extracted the inundated areas, which must be useful for flood monitoring. Erdelj et al.  
289 (2017) proposed a system that incorporates multiple RPAS devices with wireless sensor networks to  
290 perform the real-time assessment of a flood disaster. They discussed the technical strategies for the real-  
291 time flood disaster management including the detection, localization, segmentation, and size evaluation of  
292 flooded areas from RPAS-derived aerial images.

293

### 294 2.2.3. Post-flood changes

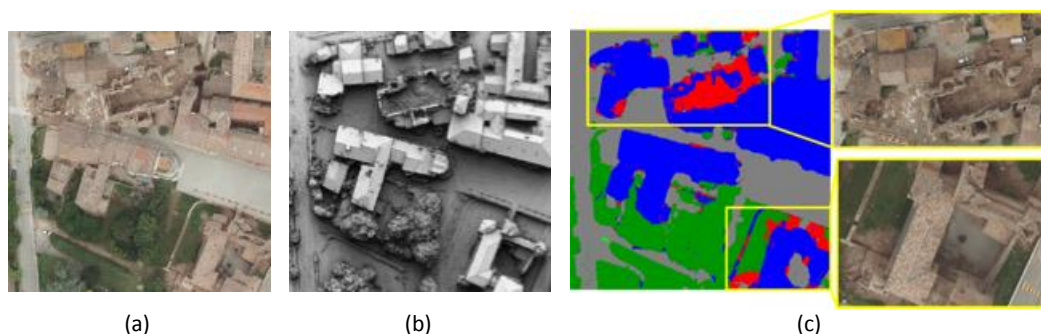
295 Post-flood assessments of the land surface materials including topography, sediment, and vegetation are  
296 more feasible by RPAS surveys. Smith et al. (2014) proposed a methodological framework for the  
297 immediate assessment of flood magnitude and affected landforms by SfM-MVS photogrammetry using  
298 both aerial and ground-based photographs. In this case, it is recommended to carefully select appropriate  
299 platforms for SfM-MVS photogrammetry (either airborne or ground-based) based on the field conditions.  
300 Tamminga et al. (2015) examined the 3D changes in river morphology by an extreme flood event, revealing  
301 that the changes in reach-scale channel patterns of erosion and deposition are poorly modelled by the 2D  
302 hydrodynamics based on the initial condition before the flood. They also demonstrate that the topographic  
303 condition can be more stable after such an extreme flood event. Langhammer et al. (2017) proposed a  
304 method to quantitatively evaluate the grain size distribution using optical images taken by a RPAS, which is  
305 applied to the sediment structure before and after a flash flood.

306 As a relatively long-term study, Dunford et al. (2009) and Hervouet et al. (2011) explored annual landscape  
307 changes after the flood using RPAS-derived images together with other datasets such as satellite image  
308 archives or a manned motor paraglider. Their work assessed the progressive development of vegetation on  
309 a braided channel at an annual scale, which appears to be controlled by local climate including rainfall,  
310 humidity, and air temperature, hydrology, groundwater level, topography, and seed availability. Changes in  
311 the sediment characteristics by a flood is another key feature to be examined.

312

## 313 2.3 Earthquakes

314 Remote sensing technology has been recognized as a suitable source to provide timely data for automated  
315 detection of damaged buildings for large areas (Dong and Shan, 2013). In the post-event, satellite images  
316 have been traditionally used for decades to visually detect the damages on the buildings to prioritize the  
317 interventions of rescuers. Operators search for externally visible damage evidence such as spalling, debris,  
318 rubble piles and broken elements, which represent strong indicators of severe structural damage. Several  
319 researches, however, have demonstrated how this kind of data often leads to the wrong detection, usually  
320 underestimating the number of the collapsed building because of their reduced resolution on the ground.  
321 In this regard, airborne images and in particular oblique acquisitions (Tu et al., 2017; Nex et al., 2014; Gerke  
322 and Kerle 2011) have demonstrated to be a better input for reliable assessments, allowing the  
323 development of automated algorithms for this task (Figure 6). The deployment of photogrammetric  
324 aeroplanes on the strike area is however very often unfeasible especially when the early (in the immediate  
325 hours after the event) damage assessment for response action is needed.



326 Figure 6. True-orthophoto, Digital Surface Model and damage map of an urban area using airborne nadir  
327 images (Source: Nex et al., 2014).

328 For this reason, RPASs have turned out to be valuable instruments for the building damage assessment. The  
329 main advantages of RPASs are their availability (and reduced cost) and the ease to repeatedly acquire high-  
330 resolution images. Thanks to their high resolution, their use is not only limited to the early impact  
331 assessment for supporting rescue operations, but it is also considered in the preliminary analysis of the  
332 structural damage assessment.

333

### 334 2.3.1 Early impact assessment

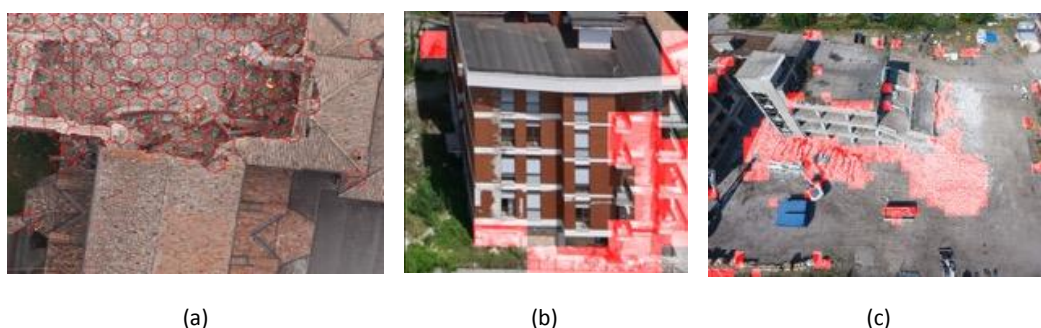
335 The fast deployment in the field, the easiness of use and the capability to provide in real time high-  
336 resolution information of inaccessible areas to prioritize the operator's activities are the strongest point of  
337 RPASs for these activities (Boccardo et al., 2015). The use of RPASs for rescue operations started almost a  
338 decade ago (Bendea et al., 2008) but their massive adoption has begun only in the very last few years  
339 (Earthquake in Nepal 2015) thanks to the development of low cost and easy to use platforms. Initiatives like  
340 *UAViators* (<http://uaviators.org/>) have further increased the public awareness and acceptance of this kind  
341 of instruments. Several rescue departments have now introduced small UAVs as part of the conventional  
342 equipment of their teams. The huge number of videos acquired by UAVs and posted by rescuers online (i.e.  
343 Youtube) after the 2016 Italian earthquakes confirm this general trend.

344 The operators use RPASs to fly over the interest area and get information through visual assessment of the  
345 streaming videos. The quality of this analysis is therefore limited to the ability of the operator to fly the  
346 RPAS over the interest area. The lack of video geo-referencing usually reduces the interpretability of the  
347 scene and the accurate localization of the collapsed parts: only small regions can be acquired in a single  
348 flight. The lack of georeferenced maps prevents the smooth sharing of the collected information with other  
349 rescue teams limiting the practical exploitation of these instruments. UAVs are mainly used in daylight  
350 conditions as the flight during the night is extremely critical, and the use of thermal images is of limited  
351 help for the rescuers.

352 Many researchers have developed algorithms to automatically extract damage information from imagery  
353 (Figure 7). The main focus of these works is to reliably detect damages in a reduced time to satisfy the time  
354 constraints of the rescuers. In (Vetrivel et al., 2015) the combined use of images and photogrammetric  
355 point clouds have shown promising results thanks to a supervised approach. This work, however,  
356 highlighted how the classifier and the designed 2D and 3D features were hardly transferable to different  
357 datasets: each scene needed to be trained independently strongly limiting the efficiency of this approach.



358 In this regard, the recent developments in machine learning (i.e. Convolutional Neural Networks, CNN)  
359 have overcome these limits (Vetrivel et al., 2017), showing how they can correctly classify scenes even if  
360 they were trained using other datasets: a trained classifier can be directly used by rescuers on the acquired  
361 images without need for further operations. The drawback of these techniques is the computational time:  
362 the use of CNN, processing like image segmentation or point cloud generation are computationally  
363 demanding and hardly compatible with real-time needs. In this regard, most recent solutions exploit only  
364 images (i.e. no need to generate point cloud) and limit the use of most expensive processes to the regions  
365 where faster classification approaches provide uncertain results to deliver an almost real-time information  
366 (Duarte et al., 2017).



367 Figure 7. Examples of damage detection on images acquired in three different scenarios (a) Mirabello (source: Vetrivel  
368 et al. 2017) and (b) L'Aquila and Lyon (source Duarte et al., 2017).

369

### 370 2.3.2 Building damage assessment

371 The damage evidence that can be captured from a UAV is not sufficient to infer the actual damage state of  
372 the building as it requires additional information such as damages to internal building elements (e.g.,  
373 columns and beams) that cannot be directly defined from images. Even though this information is limited,  
374 images can provide useful information about the external condition of the structure, evidencing anomalies  
375 and damages and providing a first important information for structural engineers. Two main typologies of  
376 investigations can be performed: (i) the use of images for the detection of cracks or damages on the  
377 external surfaces of the building (i.e. walls and roofs) and (ii) the use of point clouds (generated by  
378 photogrammetric approach) to detect structural anomalies like tilted or deformed surfaces. In both cases,  
379 the automated processing can only support and ease the work of the expert who still interprets and assess  
380 the structural integrity of the building.

381 In (Fernandez-Galarreta et al., 2015) a comprehensive analysis of both point clouds and images to support  
382 the ambiguous classification of damages and their use for damage score was presented. In this paper, the  
383 use of point clouds was considered efficient for more serious damages (partial or complete collapse of the  
384 building), while images were used to identify smaller damages like cracks that can be used as the basis for  
385 the structural engineering analysis. The use of point clouds is investigated in (Dominici et al., 2017): this  
386 contribution highlights how point clouds from UAVs can provide very useful information to detect  
387 asymmetries and small deformations of the structure.

388



## 389 2.4 Volcanic activity

390

391 RPAS is particularly advantageous when the target area of measurement is hardly accessible on the ground  
392 due to dangers of volcanic gas or risks of eruption in volcanic areas (Andrews, 2015). Although an  
393 equipment of RPAS can be lost or damaged by the volcanic activities, the operator can safely stay in a  
394 remote place. Various sensors can be mounted on a RPAS to monitor volcanic activities including  
395 topography, land cover, heat, gas composition, and even gravity field (Saiki and Ohba, 2010; Deurloo et al.,  
396 2011; Middlemiss et al., 2016). The photogrammetric approach to obtain topographic data is widely applied  
397 because RGB camera sensors are small enough to be mounted on a small aircraft. Larger aircrafts with a  
398 payload of kilograms are also utilized to mount other types of sensors to monitor various aspects of  
399 dynamic volcanic activities.

400

### 401 2.4.1. Topographic measurements of volcanoes

402 Long-distance flight of a RPAS enables quick and safe measurements of an emerging volcanic island. Tobita  
403 et al. (2014a) successfully performed a fixed-wing RPAS flight for a one-way distance of 130 km in total  
404 flight time of 2 hours and 51 minutes over the sea to capture aerial images of a newly formed volcanic  
405 island next to Nishinoshima Island (Ogasawara Islands, southwest Pacific). They performed SfM-MVS  
406 photogrammetry of the aerial images taken back from the RPAS to generate a 2.5 m resolution DEM of the  
407 island. The team also performed two successive measurements of Nishinoshima Island in the following 104  
408 days, revealing the morphological changes in the new island covering a 1,600 m by 1,400 m area (Nakano et  
409 al., 2014; Tobita et al., 2014b).

410 Since the volcanic activities often last for a long period, it is also important to connect the recent volcanic  
411 morphological changes to those in the past. Although detailed morphological data of volcanic topography is  
412 often unavailable, historical aerial photographs taken in the past decades can be utilized to generate  
413 topographic models at a certain resolution. Some case studies have used archival aerial photographs in  
414 volcanoes for periods of more than 60 years, generating DEMs with resolutions of several meters for areas  
415 of 10 km<sup>2</sup> (Gomez, 2014; Darrien et al., 2015; Gomez et al. 2015). Although these DEMs are coarser than  
416 those derived from RPAS, they can be used as supportive datasets for the modern morphological  
417 monitoring using RPAS at a higher resolution and measurement frequency.

418

### 419 2.4.2. Gas monitoring and product sampling

420 Caltabiano et al. (2005) proposed the architecture of a RPAS for the direct monitoring of gas composition in  
421 volcanic clouds of Mt. Etna in Italy. In this system, the 2-m wide fixed-wing RPAS can fly autonomously up  
422 to 4000 m altitude with a speed of 40 km/h. Like this system, a RPAS with a payload of several kilograms  
423 can carry multiple sensors to monitor different compositions of volcanic gas. McGonigle et al. (2008) used a  
424 RPAS for volcanic gas measurements at La Fossa crater of Mt. Vulcano in Italy. The RPAS has 3 kg payload  
425 and allows to host an ultraviolet spectrometer, an infrared spectrometer, and an electrochemical sensor on  
426 board. The combination of these sensors enabled the estimation of the flux of SO<sub>2</sub> and CO<sub>2</sub>, which are  
427 crucial for revealing the geochemical condition of erupting volcanoes. The monitoring of gas composition  
428 including CO<sub>2</sub>, SO<sub>2</sub>, H<sub>2</sub>S, H<sub>2</sub>, as well as the air temperature, can be used for the quantification of the



429 degassing activities and prediction of the conduit magma convection, as suggested by the test at Mt.  
430 Kirishima in Japan (Shinohara, 2013).

431 A RPAS can also transport a small ground-running robot (Unmanned Ground Vehicle: UGV) to slope head of  
432 an active volcano, where the UGV takes close-range photographs of volcanic ash on the ground surface by  
433 running down the slope (Nagatani et al., 2013). Protocols for direct sampling of volcanic products using a  
434 RPAS have also been developed (Yajima et al., 2014).

435

### 436 2.4.3. Geothermal monitoring

437 In New Zealand, Harvey et al. (2016) and Nishar et al. (2016) carried out experimental studies on the  
438 regular monitoring of intense geothermal environments using a small RPAS. They used thermal images  
439 taken by an infrared imaging sensor together with normal RGB images for photogrammetry, mapping both  
440 the ground surface temperature with detailed topography and land cover data. Chio and Lin (2017) further  
441 assessed the use of a RPAS equipped with a thermal infrared sensor for the high-resolution geothermal  
442 image mapping in a volcanic area in Taiwan. They improved the measurement accuracies using an onboard  
443 sensor capable of post-processed kinematic GNSS positioning. This allows accurate mapping with less  
444 ground control points, which are hard to place on such intense geothermal fields.

445

## 446 2.5 Wildfires

447 Wildfires are a phenomenon with local and global effects (Filizzola et al., 2017). Wildfires represent a  
448 serious threat for land managers and property owners; in the last few years, this threat has significantly  
449 expanded (Peters et al., 2013). The literature also suggests that climate change will continue to enhance  
450 the potential forest fire activity in different regions of the world (McKenzie et al. 2014; Abatzoglou and  
451 Williams, 2016). Remote sensing technologies can be very useful in monitoring such hazard (Shroeder et al.,  
452 2016). Several scientists in the last few years used satellites in fire monitoring (Shroeder et al., 2016). More  
453 recently UAVs have been considered to be useful as well. Hinkley and Zajkowski (2011) presented the  
454 results of a collaborative partnership between NASA, and the US Forest Service established for testing  
455 thermal image data for wildfires monitoring. A small unmanned airborne system served as a sensor  
456 platform. The outcome was an improved tool for wildfire decision support systems. Merino et al. (2012)  
457 described a system for forest fire monitoring using a UAS. The system integrates the information from the  
458 fleet of different vehicles to estimate the evolution of the forest fire in real time. The field tests indicated  
459 that UAS could be very helpful for the activities of firefighting (e.g. monitoring). Indeed they cover the gap  
460 between the spatial scales given by satellites and those based on cameras. Wing et al. (2014) underlined  
461 the fact that spectral and thermal sensors mounted in UAVs may hold great promise for future remote  
462 sensing applications related to forest fires. UASs have greater potential to provide enhanced flexibility for  
463 positioning and repeated data collection. Tang and Shao (2015) summarize various approaches of remote  
464 drone sensing to surveying forests, mapping canopy gaps, measuring forest canopy height, tracking forest  
465 wildfires, and supporting intensive forest management. These authors underlined the usefulness in using  
466 drones for wildfire monitoring. UAVs can repeatedly fly to record the extent of an ongoing wildfire without  
467 jeopardizing crews' safety. Zajkowski et al. (2015) tested different UAVs (e.g. quadcopter, single wing) for  
468 the analysis of fire activity. Measurements included visible and long-wave infrared (LWIR) imagery, black  
469 carbon, air temperature, relative humidity and three-dimensional wind speed and direction. The authors  
470 also described in detail the mission's plan, including the logistics of integrating RPAS into a complex



471 operations environment, specifications of the aircraft and their measurements, execution of the missions  
472 and considerations for future missions. Allison et al. (2016) provided a detailed state of the art on fire  
473 detection using both manned and unmanned aerial platforms. This review highlighted the following  
474 challenges: the need to development of robust automatic detection algorithms, the integration of sensors  
475 of varying capabilities and modalities, the development of best practices for the use of new sensor  
476 platforms (e.g. small UAVs), and their safe and effective operation in the airspace around a fire.

477

### 478 **3. Discussion and conclusion**

479 In this paper, we analysed possible applications of RPAS to natural hazards. The available literature on this  
480 topic is strongly increased in last few years, according to the improvement of the diffusion of these  
481 systems. In particular, we considered: landslides, floods, earthquakes, volcanic activities and wildfires.

482 RPAS can support studies on active geological processes and can be considered a good solution for the  
483 identification of effects and damages due to several catastrophic events. One of the most important  
484 elements that characterized the use of RPAS is their flexibility and versatility, largely confirmed by the wide  
485 number of operative solutions available in the literature. The available literature pointed out the necessity  
486 of the development of dedicated methodologies that can be able to take the full advantage of RPAS. In  
487 particular, typical results of structure from motion software (orthophoto and DSM) that are considered the  
488 end of standard data-processing, can be very often the starting point of dedicated procedures specifically  
489 conceived for natural hazards applications.

490 In the pre-emergency phase, one of the main advantages of RPAS surveys is to acquire high resolution and  
491 low-cost data to analyse and interpret environmental characteristics and potential triggering factors (e.g.  
492 slope, lithology, geostructure, land use/land cover, rock anomalies, and displacement). The data can be  
493 collected with high revisit times to obtain multi-temporal observations. After the characterization of hazard  
494 potential and vulnerability, some areas can be identified by a higher level of risk. These cases request an  
495 intensive monitoring, to gain a quantitative evaluation of the potential occurrence of an event. In this  
496 context, the use of aerial data represents a very useful complementary data source concerning the  
497 information acquired through ground-based observations in particular for dangerous areas.

498 During the emergency phase, high-resolution imagery is asked to be acquired over the event site. The  
499 primary use of this data is for the assessment of the damage grade (extent, type and damage grades  
500 specific to the event and eventually of its evolution). They may also provide relevant information that is  
501 specific to critical infrastructures, transport systems, aid and reconstruction logistics, government and  
502 community buildings, hazard exposure, displaced population, etc. Concurrently, the availability of clear and  
503 straightforward raster and vector data, integrated with base cartographic contents (transportation, surface  
504 hydrology, boundaries, etc.) it is recognized as an added-value to support decision makers for the  
505 management of emergency operations. These applications very often need prompt and reliable  
506 interventions. RPAS should, therefore, deliver information promptly. In this regard, very few researchers  
507 have focused on this issue: most of the reported work present (often time-consuming and even manual)  
508 post-processing of the acquired data, precluding the use of their results from practical and real-life  
509 scenarios. A big effort should be taken by the research community to propose faster and automated  
510 approaches.



511 As in many other domains, RPAS present a disruptive technology where, beside conventional SfM  
512 applications for 3D reconstructions, many dedicated and advanced methodologies are still in their  
513 experimental phase and will need to be further developed in the incoming years. In the following years, it  
514 would be desirable to witness the transfer of the best practices in the use of RPAS be then from the  
515 Research community to Government Agencies (or private companies) involved in the prevention and  
516 reduction of impacts of natural hazards. The Scientific community should contribute to the definition of  
517 standard methodologies that can be assumed by civil protection agencies for the management of  
518 emergencies.





## 519 **References**

- 520 Abatzoglou, J.T. and Williams, A.P.: Impact of anthropogenic climate change on wildfire across western US  
521 forests, *PNAS*, 113 (42), 11770-11775, 2016.
- 522 Astuti, G., Giudice, G., Longo, D., Melita, C. D., Muscato, G. and Orlando, A.: An overview of the “Volcan  
523 project”: An UAS for Exploration of volcanic environments, *J Intell. Robot Syst.*, 54, 471-494, 2009.
- 524 Aicardi, I., Chiabrande, F., Lingua, A., Noardo, F., Piras, M. and Vigna, B.: A methodology for acquisition and  
525 processing of thermal data acquired by UAVs: a test about subfluvial springs’ investigations, *Geomatics*,  
526 *Natural Hazards and Risk*. 8:1, 5-17, 2017. DOI: 10.1080/19475705.2016.1225229
- 527 Allison R.S., Johnston J.M., Craig G. and Jennings S.: Airborne Optical and Thermal Remote Sensing for  
528 Wildfire Detection and Monitoring Sensors, 16(8), 1310, 2016. doi:10.3390/s16081310
- 529 Andrews, C.: Pressure in the danger zone [volcanoes], *Eng. Technol.*, 10(7), 56–61,  
530 doi:10.1049/et.2015.0720, 2015.
- 531 Ardizzone, F., Fiorucci, F., Santangelo, M., Cardinali, M., Mondini, A.C., Rossi, M., Reichenbach, P., and  
532 Guzzetti, F.: Very-high resolution stereoscopic satellite images for landslide mapping. C. Margottini, P.  
533 Canuti, K. Sassa (Eds.), *Landslide Science and Practice, Landslide Inventory and Susceptibility and Hazard*  
534 *Zoning*, 1, Springer, Heidelberg, Berlin, New York, 95–101, [https://doi.org/10.1007/978-3-642-31325-7\\_12](https://doi.org/10.1007/978-3-642-31325-7_12),  
535 2013.
- 536 Ayoub, F., LePrince, S. and Keene, L.: User’s Guide to Cosis-Corr: Co-Registration of Optically Sensed Images  
537 and Correlation; California Institute of Technology: Pasadena, CA, USA, pp. 38, 2009.
- 538 Baldo M., Bicchocchi C., Chiocchini U., Giordan D. and Lollino G.: LIDAR monitoring of mass wasting processes:  
539 The Radicofani landslide, Province of Siena, Central Italy, *Gemorphology*, 105, 193-201, 2009. DOI:  
540 10.1016/j.geomorph.2008.09.015
- 541 Baiocchi, V., Dominici, D. and Mormile, M.: UAV application in post –seismic environment”, *International*  
542 *Archives of the Photogrammetry, Remote Sensing and Spatial Information Sciences*, Volume XL-1/W2, UAV-  
543 g2013, 4 – 6 September 2013, Rostock, Germany, pp. 21-25, 2013.
- 544 Bendea, H., Boccardo, P., Dequal, S., Tondo, G., Marenchino, D. and Piras, M.: Low cost UAV for post-  
545 disaster assessment. *Int. Arch. Photogramm. Remote Sens. Spat. Inf. Sci.*, 37, 1373–1379, 2008.
- 546 Boccardo, P., Chiabrande, F., Dutto, F., Tonolo, F.G. and Lingua, A.: UAV deployment exercise for mapping  
547 purposes: Evaluation of emergency response applications, *Sensors*, 15(7), 15717-15737, 2015.
- 548 Bolognesi, M., Farina, G., Alvisi, S., Franchini, M., Pellegrinelli, A. and Russo, P.: Measurement of surface  
549 velocity in open channels using a lightweight remotely piloted aircraft system. *Geomatics, Natural Hazards*  
550 *and Risk*, 8:1, 73.86, 2016. DOI: 10.1080/19475705.2016.1184717
- 551 Brardinoni, F., Slaymaker, O., and Hassan, M.A.: Landslides inventory in a rugged forested watershed: a  
552 comparison between air-photo and field survey data, *Geomorphology*, 54, 179-196,  
553 [https://doi.org/10.1016/S0169-555X\(02\)00355-0](https://doi.org/10.1016/S0169-555X(02)00355-0), 2003.



- 554 Brostow, G.J., Shotton, J., Fauqueur, J. and Cipolla, R.: Segmentation and Recognition Using Structure from  
555 Motion Point Clouds. Proc. 10th European Conf. on Computer Vision: Part I, 44–57, 2008. DOI:10.1007/978-  
556 3-540-88682-2\_5]
- 557 Caltabiano, D., Muscato, G., Orlando, A., Federico, C., Giudice, G. and Guerrieri, S.: Architecture of a UAV  
558 for volcanic gas sampling, in 2005 IEEE Conference on Emerging Technologies and Factory Automation, 1,  
559 739-744, 2005.
- 560 Carvajal, F., Agüera, F. and Pérez, M.: Surveying a landslide in a road embankment using Unmanned Aerial  
561 Vehicle photogrammetry, ISPRS Arch., 38, 1-6, 2011.
- 562 Casagli N., Frodella, W., Morelli, S., Tofani, V., Ciampalini, A., Intrieri, E., Raspini, F., Rossi, G., Tanteri, L. and  
563 Lu, P.: Spaceborne, UAV and ground-based remote sensing techniques for landslide mapping, monitoring  
564 and early warning, Geoenvironmental Disasters, 4(9), 1-23, DOI 10.1186/s40677-017-0073-1, 2017.
- 565 Chio, S.-H. and Lin, C.-H.: Preliminary Study of UAS Equipped with Thermal Camera for Volcanic Geothermal  
566 Monitoring in Taiwan, Sensors, 17(7), 1649, doi:10.3390/s17071649, 2017.
- 567 Costa, D., Burlando, P. and Priadi, C.: The importance of integrated solutions to flooding and water quality  
568 problems in the tropical megacity of Jakarta, Sustain. Cities Soc., 20, 199–209,  
569 doi:10.1016/j.scs.2015.09.009, 2016.
- 570 Filizzola, C., Corrado, R., Marchese, F., Mazzeo, G., Paciello, R., Pergola, N. and Tramutoli, V.: RST-FIRES, an  
571 exportable algorithm for early-fire detection and monitoring: Description, implementation, and field  
572 validation in the case of the MSG-SEVIRI sensor, Remote Sensing of Environment Volume, 192, 2-25, 2017.
- 573 Chou, T.Y., Yeh, M.L., Chen, Y. and Chen, Y.H.: Disaster monitoring and management by the unmanned  
574 aerial vehicle technology. Int. Archives of Photogrammetry, Remote Sensing and Spatial Information  
575 Sciences, 38(7B), 137-142, 2010.
- 576 DeBell, L., Anderson, K., Brazier, R. E., King, N. and Jones, L.: Water resource management at catchment  
577 scales using lightweight UAVs: current capabilities and future perspectives, J. Unmanned Veh. Syst., 4(1), 7–  
578 30, doi:10.1139/juvs-2015-0026, 2016.
- 579 Deffontaines, B., Chang, K.J., Champenois, J., Fruneau, B., Pathier, E., Hu, J.C., Lu, S.T. and Liu Y.C.: Active  
580 interseismic shallow deformation of the Pingting terraces (Longitudinal Valley – Eastern Taiwan) from UAV  
581 high-resolution topographic data combined with InSAR time series. Geomatics, Natural Hazards and Risk,  
582 8(1), 120-136, 2017.
- 583 Delacourt, C., Allemand, P., Jaud, M., Grandjean, P., Deschamps, A., Ammann, J., Cuq, V. and Suanes, S.:  
584 DRELIO: An Unmanned Helicopter for Imaging Coastal Areas. J. Coast. Res. 56, 1489-1493, 2009.
- 585 Deurloo, R., Bastos, L. and Bos, M.: On the Use of UAVs for Strapdown Airborne Gravimetry, pp. 255–261,  
586 Springer, Berlin, Heidelberg., 2012.
- 587 Dominici, D., Alicandro, M., Massimi, V.: UAV photogrammetry in the post-earthquake scenario: case  
588 studies in L'Aquila. Geomatics, Natural Hazards and Risk, 8(1), 87-103, 2017.
- 589 Dong, L., Shan, J.: A comprehensive review of earthquake-induced building damage detection with remote  
590 sensing techniques. ISPRS Journal of Photogrammetry and Remote Sensing, 84, pp. 85-99, 2013.



- 591 Duarte, D., Nex, F., Kerle, N., Vosseman, G.: Towards a more efficient detection of earthquake induced facad  
592 damages using oblique UAV imagery. *International Archives of the Photogrammetry, Remote Sensing and*  
593 *Spatial Information Sciences*. To be published. 2017.
- 594 Dunford, R., Michel, K., Gagnage, M., Piégay, H. and Trémelo M.-L.: Potential and constraints of Unmanned  
595 Aerial Vehicle technology for the characterization of Mediterranean riparian forest, *International Journal of*  
596 *Remote Sensing*, 30, 4915-4935, 2009.
- 597 Erdelj, M., Król, M. and Natalizio, E.: Wireless Sensor Networks and Multi-UAV systems for natural disaster  
598 management, *Comput. Networks*, 124, 72–86, doi:10.1016/j.comnet.2017.05.021, 2017.
- 599 Feng, Q., Liu, J. and Gong, J.: Urban Flood Mapping Based on Unmanned Aerial Vehicle Remote Sensing and  
600 Random Forest Classifier—A Case of Yuyao, China, *Water*, 7(4), 1437–1455, doi:10.3390/w7041437, 2015.
- 601 Fernandez Galarreta, J., Kerle, N. and Gerke, M. UAV - based urban structural damage assessment using  
602 object - based image analysis and semantic reasoning. In: *Natural hazards and earth system sciences*  
603 (NHES) : open access, 15(6) pp. 1087-1101, 2015.
- 604 Filizzola, C., Corrado, R., Marchese, F., Mazzeo, G., Paciello, R., Pergola, N. and Tramutoli, V.: RST-FIRES, an  
605 exportable algorithm for early-fire detection and monitoring: Description, implementation, and field  
606 validation in the case of the MSG-SEVIRI sensor, *Remote Sensing of Environment*, 192, 2-25, 2017.
- 607 Fiorucci, F., Giordan, D., Santangelo, M., Dutto, F., Rossi, M., and Guzzetti, F.: Criteria for the optimal  
608 selection of remote sensing images to map event landslides, *Nat. Hazards Earth Syst. Sci. Discuss.*,  
609 <https://doi.org/10.5194/nhess-2017-111>, in review, 2017
- 610 Fonstad, M.A., Dietrich, J.T., Courville, B.C., Jensen J.L. and Carbonneau, P.E.: Topographic structure from  
611 motion: a new development in photogrammetric measurement, *Earth Surf. Process. Landforms*, 38, 421-  
612 430, 2013.
- 613 Gerke, M. and Kerle, N.: Automatic structural seismic damage assessment with airborne oblique pictometry  
614 imagery. In: *PE&RS = Photogrammetric Engineering and Remote Sensing*, 77(9) pp. 885-898, 2011.
- 615 Giordan, D., Manconi, A., Facello, A., Baldo, M., dell'Anese, F., Allasia, P. and Dutto, F.: Brief Communication  
616 "The use of UAV in rock fall emergency scenario", *Nat. Hazards Earth Syst. Sci.*, 15, 163-169, 2015a.
- 617 Giordan, D., Manconi, A., Tannant, D. and Allasia, P.: UAV: low-cost remote sensing for high-resolution  
618 investigation of landslides. *IEEE International Symposium on Geoscience and Remote Sensing IGARSS*, 26-31  
619 July 2015, Milan, Italy, 5344-5347, 2015b.
- 620 Giordan, D., Allasia, P., Manconi, A., Baldo, M., Santangelo, M., Cardinali, M., Corazza, A., Albanese, V.,  
621 Lollino, G., and Guzzetti, F.: Morphological and kinematic evolution of a large earthflow: The Montaguto  
622 landslide, southern Italy, *Geomorphology*, 187, 61-79, 2013.
- 623 GSI: Information on the 2017 Northern Kyushu Heavy Rain, *Geospatial Inf. Auth. Japan* [online] Available  
624 from: [http://www.gsi.go.jp/BOUSAI/H29hukuoka\\_ooita-heavyrain.html](http://www.gsi.go.jp/BOUSAI/H29hukuoka_ooita-heavyrain.html) (Accessed 16 September 2017),  
625 2017.
- 626 Guzzetti F., Reichenbach P., Cardinali M., Galli M. and Ardizzone F.: Probabilistic landslide hazard  
627 assessment at the basin scale, *Geomorphology*, 72(1-4), 272-299, 2005.



- 628 Haneberg, W. C.: Using close range terrestrial digital photogrammetry for 3-D rock slope modeling and  
629 discontinuity mapping in the United States, *Bulletin of Engineering Geology and the Environment*, 67(4),  
630 457-469, 2008.
- 631 Harvey, M. C., Rowland, J. V. and Luketina, K. M.: Drone with thermal infrared camera provides high  
632 resolution georeferenced imagery of the Waikite geothermal area, New Zealand, *J. Volcanol. Geotherm.*  
633 *Res.*, 325, 61–69, doi:10.1016/j.jvolgeores.2016.06.014, 2016.
- 634 Heller, J., Havlena, M., Sugimoto, A. and Pajdla, T.: Structure-from-Motion Based Hand-Eye Calibration  
635 Using  $L_\infty$  Minimization. *CVPR*, 3497-3503, 2011.
- 636 Hinkley, E. and Zajkowski, T.: USDA forest service-NASA: unmanned aerial systems demonstrations—  
637 pushing the leading edge in fire mapping, *Geocarto Int.*, 26(2), 103-111, 2011.
- 638 Hunag H., Long J., Lin H., Zang L., Yi W. and Lei B.: Unmanned aerial vehicle based remote sensing method  
639 for monitoring a steep mountainous slope in the Three Gorges Reservoir, China, *Earth Science Informatics*  
640 10 (3) 287-301, 2017.
- 641 Immerzeel, W.W., Kraaijenbrink, P. D. A., Shea, J. M., Shrestha, A. B., Pellicciotti, F., Bierkens, M. F. P. and  
642 de Jonga, .S.M.: High-resolution monitoring of Himalayan glacier dynamics using unmanned aerial vehicles,  
643 *Remote Sensing of Environment*, 150, 93-103, 2014.
- 644 Irschara, A., Zach, C., Frahm, J. M. and Bischof, H.: From Structure-from-Motion Point Clouds to Fast  
645 Location Recognition, *CVPR*, 2599-2606, 2009.
- 646 Jaud, M.; Grasso, F.; Le Dantec, N.; Verney, R.; Delacourt, C.; Ammann, J.; Deloffre, J.; Grandjean, P.  
647 Potential of UAVs for Monitoring Mudflat Morphodynamics (Application to the Seine Estuary, France).  
648 *ISPRS Int. J. Geo-Inf.* 5(4), 50, 2016.
- 649 Joyce K. E., Belliss, S. E., Samsonov, S. V., McNeill, S. J. and Glassey, P. J.: A review of the status of satellite  
650 remote sensing and image processing techniques for mapping natural hazards and disasters. *Progress in*  
651 *Physical Geography*, 33, 83-207, 2009.
- 652 Jurecka, M. and Niedzielski, T.: A procedure for delineating a search region in the UAV-based SAR activities.  
653 *Geomatics, Natural Hazards and Risk*, 8(1), 53-72, 2017.
- 654 Klemas, V. V.: Coastal and Environmental Remote Sensing from Unmanned Aerial Vehicles: An Overview,  
655 *Journal of Coastal Research*, 31(5), 1260-1267, 2015.
- 656 Koutsoudisa, A., Vidmarb, B., Ioannakisa, G., Arnaoutogloua, F., Pavlidis, V. and Chamzasc, C.: Multi-image  
657 3D reconstruction data evaluation, *Journal of Cultural Heritage*, 15, 73-79, 2014.
- 658 Lazzari, M. and Gioia D.: UAV images and high-resolution DEMs for geomorphological analysis and hazard  
659 evaluation: the case of the Uggiano archaeological site (Ferrandina, southern Italy). *Geomatics, Natural*  
660 *Hazards and Risk*, 8(1), 104-119, 2017.
- 661 Langhammer, J., Lendziach, T., Miřijovskỳ, J. and Hartvich, F.: UAV-based optical granulometry as tool for  
662 detecting changes in structure of flood depositions, *Remote Sens.*, 9(3), doi:10.3390/rs9030240, 2017.
- 663 Le Coz, J., Patalano, A., Collins, D., Guillén, N. F., García, C. M., Smart, G. M., Bind, J., Chiaverini, A., Le  
664 Boursicaud, R., Dramais, G. and Braud, I.: Crowdsourced data for flood hydrology: Feedback from recent



- 665 citizen science projects in Argentina, France and New Zealand, *J. Hydrol.*, 541, 766–777,  
666 doi:10.1016/j.jhydrol.2016.07.036, 2016.
- 667 Leprince, S.: Monitoring earth surface dynamics with optical imagery, *EOS Trans. Am. Geophys. Union* 89, 1-  
668 2, 2008.
- 669 Leprince, S., Barbot, S., Ayoub, F. and Ayoub, J.P.: Automatic and precise orthorectification, co-  
670 registration, and sub-pixel correlation of satellite images, application to ground deformation  
671 measurements. *IEEE Trans. Geosci. Remote Sens.* 46, 1529-1558, 2007.
- 672 Li, Y., Gong, J. H., Zhu, J., Ye, L., Song, Y. Q. and Yue, Y. J.: Efficient dam break flood simulation methods for  
673 developing a preliminary evacuation plan after the Wenchuan Earthquake, *Nat. Hazards Earth Syst. Sci.*,  
674 12(1), 97–106, doi:10.5194/nhess-12-97-2012, 2012.
- 675 Lucieer, A., de Jong S. M. and Turner, D.: Mapping landslide displacements using Structure from Motion  
676 (SfM) and image correlation of multi-temporal UAV photography, *Progress in Physical Geography*, 38(1),  
677 97–116, 2014a.
- 678 Lucieer, A., Turner, D., King, D. H. and Robinson, S. A.: Using an Unmanned Aerial Vehicle (UAV) to capture  
679 microtopography of Antarctic moss beds. *International Journal of Applied Earth Observation and  
680 Geoinformation*. 27(a), 53–62, 2014b.
- 681 Manfredini, A.M.: A Methodology for the Promotion of Cultural Heritage Sites Through the Use of Low-Cost  
682 Technologies and Procedures. In: *proc. 17th Int. Conf. on 3D Web Technology Los Angeles, CA, August 4-5,*  
683 *2012*, 180, 2012.
- 684 Martin, P. G., Smith, N. T., Yamashiki, Y., Payton, O. D., Russell-Pavier F. S., Fardoulis, J. S., Richards D. A.  
685 and Scott T. B.: 3D unmanned aerial vehicle radiation mapping for assessing contaminant distribution and  
686 mobility, *International Journal of Applied Earth Observation and Geoinformation*, 52, 12-19, 2016.
- 687 Marek, L., Miřijovský, J. and Tuček, P.: Monitoring of the Shallow Landslide Using UAV Photogrammetry and  
688 Geodetic Measurements, In: Lollino G., Giordan D., Crosta G.B., Corominas J., Azzam R. Wasowski J., Sciarra  
689 N. (eds.) *Engineering Geology for Society and Territory – Landslide Processes*, Springer International  
690 Publishing Switzerland, 2, 113-116, 2015.
- 691 Martínez-de Dios, J.R., Merino, L., Caballero, F. and Ollero, A.: Automatic forest-fire measuring using ground  
692 stations and unmanned aerial systems. *Sensors*, 11(6), 6328-6353, 2011.
- 693 McKenzie, D., Shankar, U., Keane, R. E., Stavros, E. N., Heilman, W. E., Fox, D. G. and Riebau, A. C.: Smoke  
694 consequences of new wildfire regimes driven by climate change, *Earth's Future*, 2(2), 35-59, 2014.
- 695 Merino, L., Caballero, F., Martínez-de-Dios, J.R., Iván, M. and Aníbal, O.: An unmanned aircraft system for  
696 automatic forest fire monitoring and measurement, *J. Intell. Rob. Syst.*, 65(1-4), 533-548, 2012.
- 697 McGonigle, A. J. S., Aiuppa, A., Giudice, G., Tamburello, G., Hodson, A. J. and Gurrieri, S.: Unmanned aerial  
698 vehicle measurements of volcanic carbon dioxide fluxes, *Geophys. Res. Lett.*, 35(6), 3–6,  
699 doi:10.1029/2007GL032508, 2008.
- 700 Middlemiss, R.P., Samarelli, A., Paul, D.J., Hough, J., Rowan, S. and Hammond, G.D.: The First Measurement  
701 of the Earth Tides with a MEMS Gravimeter, *Nature*, 531(1), 614, 2016.



- 702 Molina, P., Colomina, I., Vitoria, T., Silva, P.F., Skaloud, J., Kornus, W., Prades, R. and Aguilera, C.: Searching  
703 lost people with UAVs: the system and results of the close-search project. *International Archives of the*  
704 *Photogrammetry, Remote Sensing and Spatial Information Sciences*, 39(B1), 441-446, 2012.
- 705 Moslah, O., Guitteny, V., Couvet, S.: Geo-referencing Uncalibrated Photographs Using Aerial Images and 3D  
706 Urban Models. *CORESA*, 1–5, 2009.
- 707 Murphy, R. R., Steimle, E., Griffin, C., Cullins, C., Hall, M. and Pratt, K.: Cooperative use of unmanned sea  
708 surface and micro aerial vehicles at Hurricane Wilma, *Journal of Field Robotics*, 25(3), 164-180, 2008.
- 709 Nagatani, K., Akiyama, K., Yamauchi, G., Otsuka, H., Nakamura, T., Kiribayashi, S., Yoshida, K., Hada, Y., Yuta,  
710 S., Fujino, K., Izu, T. and Mackay, R.: Volcanic ash observation in active volcano areas using teleoperated  
711 mobile robots - Introduction to our robotic-volcano-observation project and field experiments, in: *proc.*  
712 *2013 IEEE International Symposium on Safety, Security, and Rescue Robotics (SSRR)*, Linköping, Sweden, 21-  
713 26 Oct. 2013, 1–6, 2013.
- 714 Nakano, T., Kamiya, I., Tobita, M., Iwahashi, J. and Nakajima, H.: Landform monitoring in active volcano by  
715 UAV and SFM-MVS technique, *Int. Arch. Photogramm. Remote Sens. Spat. Inf. Sci. - ISPRS Arch.*, 40(8), 71–  
716 75, 2014.
- 717 Nassar, K., Aly, E.A. and Jung, Y.: Structure-from-Motion for Earthwork Planning, in: *proc. of 28th ISARC*  
718 *2011*, Seoul, Korea, 310–316, 2011.
- 719 Nex, F., Rupnik, E., Toschi, I., Remondino, F., 2014. Automated processing of high resolution airborne  
720 images for earthquake damage assessment. In: *International Archives of Photogrammetry and Remote*  
721 *Sensing and Spatial Information Sciences*, Vol. XL-1.
- 722 Niculiță, M.: Automatic landslide length and width estimation based on the geometric processing of the  
723 bounding box and the geomorphometric analysis of DEMs, *Nat. Hazards Earth Syst. Sci.*, 16, 2021-2030,  
724 <https://doi.org/10.5194/nhess-16-2021-2016>, 2016.
- 725 Niethammer, U., James, M.R., Rothmund, S., Tranelletti, J. and Joswig, M.: UAV-based remote sensing of  
726 the Super-Sauze landslide: evaluation and results, *Eng Geol*, 128, 2-11, 2012.
- 727 Niethammer, U., Rothmund, S., James, M.R., Tranelletti, J. and Joswig, M.: UAV-based remote sensing of  
728 landslides. In *Proceedings of the International Archives of Photogrammetry, Remote Sensing and Spatial*  
729 *Information Sciences, Commission V Symposium*, Newcastle upon Tyne, UK, 21–24 June 2010, 496–501,  
730 2010.
- 731 Niethammer, U., Rothmund, S., Joswig, M.: UAV-based remote sensing of the slow-moving landslide Super-  
732 Sauze. In: Malet, J.-P., Remaître, A., Boogard, T. (Eds) *Proceedings of the International Conference on*  
733 *Landslide Processes: from geomorphologic mapping to dynamic modelling*, Strasbourg, CERIG Editions, pp.  
734 69-74, 2009.
- 735 Niethammer, U., Rothmund, S., Schwaderer, U., Zeman, J., Joswig, M.: Open Source Image-Processing Tools  
736 for Low-Cost UAV-Based Landslide Investigations. *International Archives of the Photogrammetry, Remote*  
737 *Sensing and Spatial Information Sciences, Volume XXXVIII-1/C22*, 2011 *ISPRS Zurich 2011 Workshop*, 14-16  
738 September 2011, Zurich, Switzerland, 161-166, 2011.



- 739 Nishar, A., Richards, S., Breen, D., Robertson, J. and Breen, B.: Thermal infrared imaging of geothermal  
740 environments and by an unmanned aerial vehicle (UAV): A case study of the Wairakei - Tauhara geothermal  
741 field, Taupo, New Zealand, *Renew. Energy*, 86, 1256–1264, doi:10.1016/j.renene.2015.09.042, 2016.
- 742 Peters, M. P., Iverson, L. R., Matthews, S. N. and Prasad, A. M.: Wildfire hazard mapping: exploring site  
743 conditions in eastern US wildland–urban interfaces, *International Journal of Wildland Fire*, 22, 567-578,  
744 2013.
- 745 Piras, M., Taddia, G., Forno, M.G., Gattiglio, M., Aicardi, I., Dabove, P., Lo Russo, S. and Lingua, A.: Detailed  
746 geological mapping in mountain areas using an unmanned aerial vehicle: application to the Rodoretto  
747 Valley, NW Italian Alps, *Geomatics, Natural Hazards and Risk*, 8(1), 137-149, 2017.
- 748 Pollefeys, M., Gool, L. V., Vergauwen, M., Cornelis, K., Verbiest, F. and Tops, J.: Image-Based 3D Acquisition  
749 of Archaeological Heritage and Applications. *Proc. Conf. on Virtual Reality, Archeology, and Cultural  
750 Heritage*, 255–262, 2001.
- 751 Pratt, K.S., Murphy, R., Stover, S. and Griffin, C.: Conops and autonomy recommendations for VTOL small  
752 unmanned aerial system based on Hurricane Katrina operations, *Journal of Field Robotics*, 26(8), 636-650,  
753 2009.
- 754 Rau, J.Y., Jhan, J.P., Lo, C.F. and Lin Y. S.: Landslide mapping using imagery acquired by a fixed-wing UAV,  
755 *International Archives of the Photogrammetry, Remote Sensing and Spatial Information Sciences*, Volume  
756 XXXVIII-1/C22, 2011 ISPRS Zurich 2011 Workshop, 14-16 September 2011, Zurich, Switzerland, 195-200,  
757 2011.
- 758 Razak, K. A., Santangelo, M., Van Westen, C. J., Straatsma, M. W., and de Jong, S. M.: Generating an optimal  
759 DTM from airborne laser scanning data for landslide mapping in a tropical forest environment,  
760 *Geomorphology*, 190, 112-125, 25 <https://doi.org/10.1016/j.geomorph.2013.02.021>, 2013
- 761 Ryan, J. C., Hubbard, A. L., Box, J. E., Todd, J., Christoffersen, P., Carr, j. R., Holt, T. O., and Snooke, N.:  
762 Repeat UAV photogrammetry to assess calving front dynamics at a large outlet glacier draining the  
763 Greenland Ice Sheet, *The Cryosphere*, 9, 1-11, 2015.
- 764 Saiki, K. and Ohba, T.: Development of an unmanned observation aerial vehicle (UAV) as a tool for volcano  
765 survey (in Japanese with English abstract), *Bull. Volcanol. Soc. Japan Second Ser.*, 55(3), 137–146, 2010.
- 766 Salvini, R., Mastrorocco, G., Seddaiu, M., Rossi, D. and Vanneschi, C.: The use of an unmanned aerial vehicle  
767 for fracture mapping within a marble quarry (Carrara, Italy): photogrammetry and discrete fracture  
768 network modelling, *Geomatics, Natural Hazards and Risk*, 8(1), 34-52, 2017.
- 769 Sanada, Y. And Torii T.: Aerial radiation monitoring around the Fukushima Dai-ichi nuclear power plant  
770 using an unmanned helicopter, *Journal of Environmental Radioactivity*, 139, 294-299, 2015.
- 771 Santangelo, M., Cardinali, M., Rossi, M., Mondini, A. C., and Guzzetti, F.: Remote landslide mapping using a  
772 laser rangefinder binocular and GPS, *Nat. Hazards Earth Syst. Sci.*, 10, 2539-2546,  
773 <https://doi.org/10.5194/nhess-10-2539-2010>, 2010.
- 774 Saroglou, C., Asteriou, P., Zekkos, D., Tsiambaos, G., Clark, M., and Manousakis, J.: UAV-enabled  
775 reconnaissance and trajectory modeling of a co-seismic rockfall in Lefkada, *Nat. Hazards Earth Syst. Sci.  
776 Discuss.*, <https://doi.org/10.5194/nhess-2017-29>, in review, 2017.



- 777 Scaioni, M., Longoni, L., Melillo, V. and Papini, M.: Remote Sensing for Landslide Investigations: An  
778 Overview of Recent Achievements and Perspectives, *Remote Sens.* 6(10), 9600-9652, 2014,
- 779 Schroeder, W., Oliva, P., Giglio, L., Quayle, B., Lorenz, E. and Morelli, F.: Active fire detection using Landsat-  
780 8/OLI data, *Remote Sensing of Environment*, 185, 210-220, 2016.
- 781 Şerban, G., Rus, I., Vele, D., Breţcan, P., Alexe, M. and Petrea, D.: Flood-prone area delimitation using UAV  
782 technology, in the areas hard-to-reach for classic aircrafts: case study in the north-east of Apuseni  
783 Mountains, Transylvania, *Nat. Hazards*, 82(3), 1817–1832, doi:10.1007/s11069-016-2266-4, 2016.
- 784 Shinohara, H.: Composition of volcanic gases emitted during repeating Vulcanian eruption stage of  
785 Shinmoedake, Kirishima volcano, Japan, *Earth Planets Sp.*, 65(6), 667–675, 2013.  
786 doi:10.5047/eps.2012.11.001,
- 787 Silvagni, M., Tonoli, A., Zenerino, E and Chiaberge, M.: Multipurpose UAV for search and rescue operations  
788 in mountain avalanche events. *Geomatics, Natural Hazards and Risk*, 8(1), 18-33, 2017.
- 789 Sohn, H., Heo, J., Yoo, H., Kim, S. and Cho, H.: Hierarchical multi-sensor approach for the assessment of  
790 flood related damages, *Proc. XXI Congr.*, 207–210, 2008.
- 791 Stöcker, C., Bennett, R., Nex, F., Gerke, M. and Zevenbergen, J.: Review of the current state of UAV  
792 regulations, *Remote Sensing* 9(5), 459, doi:10.3390/rs9050459, 2017.
- 793 Tang, L. and Shao, G.: Drone remote sensing for forestry research and practices. *J. For. Res.*, 26, 791-797,  
794 2015.
- 795 Tannant, D. D., Giordan, D. and Morgenroth J.: Characterization and analysis of a translational rockslide on  
796 a stepped-planar slip surface. *Engineering Geology*, 220, 144-151, 2017.
- 797 Tarolli, P.: High-resolution topography for understanding Earth surface processes: opportunities and  
798 challenges, *Geomorphology*, 216, 295–312, 2014.
- 799 Tobita, M., Kamiya, I., Iwahashi, J., Nakano, T. and Takakuwa, N.: UAV aerial photogrammetry in  
800 Nishinoshima Island and its analysis (in Japanese), *Bull. Geospatial Inf. Auth. Japan*, 125, 115–124, 2014a.
- 801 Tobita, M., Kamiya, I., Nakano, T., Iwahashi, J., Osumi, K. and Takakuwa, N.: Precise UAV aerial  
802 photogrammetry in Nishinoshima Island (in Japanese), *Bull. Geospatial Inf. Auth. Japan*, 125, 145–154,  
803 2014b.
- 804 Tokarczyk, P., Leitao, J. P., Rieckermann, J., Schindler, K. and Blumensaat, F.: High-quality observation of  
805 surface imperviousness for urban runoff modelling using UAV imagery, *Hydrol. Earth Syst. Sci.*, 19(10),  
806 4215–4228, doi:10.5194/hess-19-4215-2015, 2015.
- 807 Torrero, L. Seoli, L. Molino, A. Giordan, D. Manconi, A. Allasia, P. and Baldo, M.: The Use of Micro-UAV to  
808 Monitor Active Landslide Scenarios, in: *Engineering Geology for Society and Territory*, edited by: Lollino, G.,  
809 Manconi, A., Guzzetti, F., Culshaw, M., Bobrowsky P., and Luino, F., Springer International Publishing  
810 Switzerland, 5, 701-704, [https://doi.org/10.1007/978-3-319-09048-1\\_136](https://doi.org/10.1007/978-3-319-09048-1_136), 2015.
- 811 Török, Á., Barsi, Á., Bögöly, G., Lovas, T., Somogyi, Á., and Görög, P.: Slope stability and rock fall hazard  
812 assessment of volcanic tuffs using RPAS and TLS with 2D FEM slope modelling, *Nat. Hazards Earth Syst. Sci.*  
813 *Discuss.*, <https://doi.org/10.5194/nhess-2017-56>, in review, 2017.





- 814 Travelletti, J., Delacourt, C., Allemand, P., Malet, J.P., Schmittbuhl, J., Toussaint, R. and Bastard, M.:  
815 Correlation of multi-temporal ground-based optical images for landslide monitoring: application, potential  
816 and limitations, *ISPRS J Photogramm Remote Sens*, 70, 39-55, 2012.
- 817 Tu, J., Sui, H., Feng, W., Sun, K., Xu, C. and Han, Q.: Detecting building facade damage from oblique aerial  
818 images using local symmetry feature and the Gini Index. *Remote Sensing Letters*, 8(7), 676-685, 2017.
- 819 Turner, D. and Lucieer, A.: Using a micro unmanned aerial vehicle (UAV) for ultra-high resolution mapping  
820 and monitoring of landslide dynamics. In *Proceedings of the IEEE International Geoscience and Remote  
821 Sensing Symposium*, Melbourne, Australia, 25 July 2013.
- 822 Turner, D., Lucieer, A. and Watson, C.: An automated technique for generating georectified mosaics from  
823 ultrahigh resolution unmanned aerial vehicle (UAV) imagery, structure from motion (SfM) point  
824 clouds. *Remote Sens.*, 4(12), 1392-1410, 2012.
- 825 Turner, D., Lucieer, A. and de Jong, S.M.: Time Series Analysis of Landslide Dynamics Using an Unmanned  
826 Aerial Vehicle (UAV), *Remote Sensing*, 7(2), 1736-1757, 2015.
- 827 Van Den Eeckhaut, M., Poesen, J., Verstraeten, G., Vanacker, V., Nyssen, J., Moeyersons, J., van Beek, L. P.  
828 H., and Vandekerckhove, L.: Use of LIDAR-derived images for mapping old landslides under forest, *Earth  
829 Surf. Proc. Land.*, 32, 754-769, <https://doi.org/10.1002/esp.1417>, 2007.
- 830 Van Westen J.C., Castellanos, E. and Kuriakose S.L.: Spatial data for landslide susceptibility, hazard, and  
831 vulnerability assessment: An overview. *Engineering Geology*, 102(3-4), 112-131, 2008.
- 832 Vetrivel, A., Gerke, M., Kerle, N., Nex, F. and Vosselman, G.: Disaster damage detection through synergistic  
833 use of deep learning and 3D point cloud features derived from very high resolution oblique aerial images,  
834 and multiple-kernel-learning. *ISPRS Journal of Photogrammetry and Remote Sensing*, in Press.  
835 <https://doi.org/10.1016/j.isprsjprs.2017.03.001>.
- 836 Vetrivel, A., Gerke, M., Kerle, N. and Vosselman, G.: Identification of damage in buildings based on gaps in  
837 3D point clouds from very high resolution oblique airborne images. *ISPRS Journal of Photogrammetry and  
838 Remote Sensing*, 105, 61-78, 2015.
- 839 Walter, M., Niethammer, U., Rothmund, S. and Joswig, M.: Joint analysis of the Super-Sauze (French Alps)  
840 mudslide by nanoseismic monitoring and UAV-based remote sensing. *EAGE First Break*, 27(8), 75-82, 2009.
- 841 Wen, Q., He, H., Wang, X., Wu, W., Wang, L., Xu, F., Wang, P., Tang, T. and Lei, Y.: UAV remote sensing  
842 hazard assessment in Zhouqu debris flow disaster, in: *Remote Sensing of the Ocean, Sea Ice, Coastal  
843 Waters, and Large Water Regions*, Bostater, C.R., Ertikas, S.P., Neyt X. and Velez-Reyes, M. (eds.), , 8 pp.,  
844 2011.
- 845 Westoby, M. J., Brasington, J., Glasser, N. F., Hambrey, M. J. and Reynolds, M. J.: Structure-from-Motion  
846 photogrammetry: A low-cost, effective tool for geoscience applications. *Geomorphology*, 179, 300-314,  
847 2012.
- 848 Wing, M. G., Burnett J. D. and Sessions, J.: Remote sensing and unmanned aerial system technology for  
849 monitoring and quantifying forest fire impacts, *Int J Remote Sens Appl.*, 4(1), 18-35, 2014.



- 850 Yajima, R., Nagatani, K. and Yoshida, K.: Development and field testing of UAV-based sampling devices for  
851 obtaining volcanic products, in 2014 IEEE International Symposium on Safety, Security, and Rescue  
852 Robotics, 27-30 Oct. 2014, Hokkaido, Japan, 1–5, 2014.
- 853 Yoon, W.S., Jeong, U.J. and Kim, J.H.: Kinematic analysis for sliding failure of multi-faced rock slopes,  
854 Engineering Geology, 67, 51-61, 2002.
- 855 Zajkowski, T.J., Dickinson, M.B., Hiers, J.K., Holley, W., Williams, B.W., Paxton, A., Martinez, O. and Walker,  
856 G.W.: Evaluation and use of remotely piloted aircraft systems for operations and research – RxCADRE 2012.  
857 International Journal of Wildland Fire, 25, 114-128, 2015.
- 858 Zazo, S., Molina, J. L. and Rodríguez-González, P.: Analysis of flood modeling through innovative geomatic  
859 methods, J. Hydrol., 524, 522–537, doi:10.1016/j.jhydrol.2015.03.011, 2015.